

Rescue of Brain Function Using Tunneling Nanotubes Between Neural Stem Cells and Brain Microvascular Endothelial Cells

Xiaoqing Wang¹ · Xiaowen Yu² · Chong Xie¹ · Zijian Tan¹ · Qi Tian¹ · Desheng Zhu¹ · Mingyuan Liu¹ · Yangtai Guan^{1,3}

Received: 4 December 2014 / Accepted: 21 May 2015
© Springer Science+Business Media New York 2015

Abstract Evidence indicates that neural stem cells (NSCs) can ameliorate cerebral ischemia in animal models. In this study, we investigated the mechanism underlying one of the neuroprotective effects of NSCs: tunneling nanotube (TNT) formation. We addressed whether the control of cell-to-cell communication processes between NSCs and brain microvascular endothelial cells (BMECs) and, particularly, the control of TNT formation could influence the rescue function of stem cells. In an attempt to mimic the cellular microenvironment in vitro, a co-culture system consisting of terminally differentiated BMECs from mice in a distressed state and NSCs was constructed. Additionally, engraftment experiments with infarcted mouse brains revealed that control of TNT formation influenced the effects of stem cell transplantation in vivo. In conclusion, our findings provide the first evidence that TNTs exist between NSCs and BMECs and that regulation of TNT formation alters cell function.

Xiaoqing Wang and Xiaowen Yu devoted equally to this work.

Electronic supplementary material The online version of this article (doi:10.1007/s12035-015-9225-z) contains supplementary material, which is available to authorized users.

✉ Mingyuan Liu
liu.mingyuan@foxmail.com

✉ Yangtai Guan
yangtaiguan@sina.com

¹ Department of Neurology, Changhai Hospital, Second Military Medical University, Shanghai 200433, China

² Department of Geriatrics, Changhai Hospital, Second Military Medical University, Shanghai 200433, China

³ Department of Neurology, Ren Ji Hospital, School of Medicine, Shanghai Jiaotong University, Shanghai, China

Keywords Tunneling nanotubes · Neural stem cells · Brain microvascular endothelial cells · MCAO model

Introduction

Ischemic stroke (IS), which occurs when relevant vessels to the brain are occluded, is among the main causes of death worldwide. Approximately half of IS patients exhibit various levels of neurological damage. Standard treatment with intravenous tissue plasminogen activator (tPA) is the sole approved drug therapy for IS [1], but only a limited number of patients exhibit sufficient indications for thrombolysis with this treatment.

Although traditional therapy develops slowly, stem cell therapy has recently emerged as a promising therapeutic option for the treatment of various neurodegenerative diseases [2]. Neural stem cell (NSC) transplantation offers the following benefits for cerebral ischemia:

- These cells differentiate into other cells, such as neurons, to replace the relevant components in the ischemic area [3].
- These cells induce local angiogenesis to improve compensatory circulation and rescue ischemic regions [4].
- Paracrine factors from NSCs play an important role in antioxidation and the protection of vascular endothelial cells [5].

However, whether NSCs can improve brain function after stroke by direct contact remains unknown. Brain microvascular endothelial cell (BMEC) injuries are considered the basic impetus of ischemia/reperfusion, which enhances the release of oxygen free radicals and exacerbates brain damage [6].

Therefore, we focus on the protection of the BMECs by NSCs through mitochondrial transport via tunneling nanotubes (TNTs) [7].

In 2004 Rustom et al. [8] first reported on thin extracellular protrusions that connect cultured rat pheochromocytoma PC12 cells over long distances and act as conduits for the intercellular transfer of a range of cellular compounds. These structures are suspended above the substrate and contain a straight, continuous actin rod enclosed in a lipid bilayer. The structures were called TNTs; they are long, thin microtubule- and F-actin-containing bridges that connect two mammalian cells [9, 10]. These bridges extend up to 100 μm in length and range from 50 to 700 nm in diameter [11] due to depolymerization and the incorporation of additional components, such as microtubules, inside the TNTs. The bridges are not empty, but rather they are filled with cytoskeletal filaments that span along their entire length uniformly. TNTs have been identified in various cell types, where they form direct cell-to-cell channels [12]. Several *in vitro* studies have demonstrated that these structures facilitate the exchange of molecules, RNA, proteins, and especially mitochondria, which is reported most frequently [13].

In our experiments, we addressed the influence of the antitubulin agent nocodazole and an enhancer (TNFaip2 overexpression) [14] on TNT formation and we analyzed the potential involvement of TNT mechanisms in improved neurological function in a middle cerebral artery occlusion (MCAO) rodent model.

We provide clear evidence for the efficacy and safety of NSC therapy for IS by creating a mitochondrial passageway.

Methods and Materials

Cell Culture and Co-Culture of NSCs and BMECs

NSCs were isolated using previously described procedures [15]. BMECs were purchased from Obio Technology Co., Ltd. (Shanghai, China) and cultivated in the medium recommended by the supplier. Cells were grown in tissue culture incubators at 37 °C and 5 % CO₂. For selective inhibition of TNT formation, co-cultures were treated with nocodazole (5 \times 10⁻⁸ M, Sigma-Aldrich, St. Louis, USA).

Mitotracker, CFSE Staining and Transfection of Lentivirus

Mitotracker Red (Invitrogen Life Technologies, CA, USA) was used to visualize mitochondria. NSCs were stained with 200 nM Mitotracker Red dissolved in Dulbecco's modified Eagle's medium/F12 (DMEM/F12) for 20 min in tissue culture incubators at 37 °C. Excess dye was removed by washing with the same medium, and the cells were incubated for 2–

4 days after dyeing to prevent leakage of the dye. Then, 2.5 mM 5,6-carboxyfluorescein diacetate succinimidyl ester (CFSE, Invitrogen Life Technologies) was used to stain adherent BMEC sample in DMEM for 20 min at 37 °C. Excess dye was removed by washing with phosphate-buffered saline (PBS). Stained BMECs were detached and seeded for co-culture. M-sec or empty lentiviral infection was conducted after NSCs had been transferred via mechanical isolation, using 10 μl of virus per bottle to infect approximately 30 % of the cells.

Confocal Microscopy, TNT Counting, and Transmission Electron Microscopy

Prestained NSCs and BMECs were seeded onto glass coverslips (5000 cells/cm²). Cells were fixed with 4 % paraformaldehyde (PFA) for 30 min at RT, and the coverslips were mounted using Fluoroshield with 4',6-diamidino-2-phenylindole (DAPI, Sigma-Aldrich). Fluorescence images of the cells were obtained using a Leica TCS-SP2 confocal microscope (Leica Microsystems, Wetzlar, Germany). Five randomly selected fields of vision under confocal microscopy were used to count the number of TNTs and to calculate an average value. For the transmission electron microscopy (TEM) observation of cytology samples, a cell scraper (CORNING-COSTAR, USA) was used to carefully scrape co-cultured cells from the bottom of the cell culture bottle in each group. All of the contents from the cell culture bottle were slowly poured into an Eppendorf (EP) tube, followed by a low-speed centrifugation for 3 min. The pelleted cells were removed from the EP tube and immersed in glutaraldehyde for TEM ultramicrotomy. For brain tissue TEM observations, the tissue was cut into 1 \times 1 \times 1 mm cubes and immersed in glutaraldehyde following the same protocol for the cell samples in each group.

Animal Groups

Adult male C57 mice weighing 25 \pm 2 g (Experimental Animal Centre, Shanghai Second Military Medical University) mice were randomly assigned to four groups. Groups 1 (NSC+PBS) and 2 (NSC+NOCO) were used to compare the effects of the TNT inhibitor (nocodazole) on NSCs transplanted into animals with MCAO. Groups 3 (MSEC-NSC) and 4 (NC-NSC) were subjected to lentiviral (LV) vector infection protocols to compare the effects of a TNT enhancer (M-sec, the same for TNFaip2) on NSCs transplanted into animals with MCAO. The animals in group 1 received an intracarotid injection of 10⁶ NSCs suspended in 0.1 ml PBS, whereas the cells transplanted into the group 2 animals were pretreated with nocodazole, which has been widely used for TNT inhibition [13]. The NSCs used in group 3 were transfected with LV-M-sec, whereas the cells used in group 4 were transfected

with LV-e-GFP as a negative control (NC). All of the animals were sacrificed 1 day after the MCAO procedure.

MCAO Model and Intracarotid Transplantation of NSCs

Adult male C57 mice weighing 25 ± 2 g (Experimental Animal Centre, Shanghai Second Military Medical University) mice were subjected to MCAO for 1.5 h, as previously described, using an intraluminal filament technique [16, 17]. Briefly, anesthesia was induced via intraperitoneal administration of chloral hydrate. After the right carotid region was exposed, the external and common carotid arteries (CCAs) were permanently ligated. A microsurgical clip was placed on the internal carotid artery (ICA) near the carotid bifurcation. A catheter was inserted into the CCA through a puncture between the two suture ties with its tip placed near the carotid bifurcation. Immediately after inserting the catheter and removing the microvascular clip from the ICA, approximately 10^6 cells suspended in 0.1 ml PBS were slowly infused over a period of 5 min. After the cell delivery was complete, a microclip was placed on the ICA as described above. A 25 mm length of nylon monofilament (Beijing Cinontech Co., Ltd.) with a poly-L-lysine coated tip was introduced through the puncture site after the catheter was withdrawn. The clip was then removed to allow the filament to further advance in the ICA until resistance was felt at approximately 8–10 mm from the carotid bifurcation, thereby occluding the middle cerebral artery. After MCAO that persisted for 1.5 h, reperfusion was permitted by gently withdrawing the suture. The infarct volume, histological appearance, mitochondrial effects, biochemical analyses, and neurological deficits were evaluated 24 h after the MCAO. The Experimentation Ethics Committee of the Shanghai Second Military Medical University, China, approved the animal protocols.

Histological Assessment

Brain sections from various animal groups were paraffin-embedded; these sections were subsequently de-paraffinized, rehydrated, and subjected to Nissl staining according to a standard protocol. Stained brain sections were placed under cover slips and imaged using a light microscope.

TTC Staining

The infarct volume was assessed by staining with 2,3,5-triphenyltetrazolium chloride (TTC, Sigma-Aldrich). Animals were decapitated, and their brains were cut into 2-mm-thick coronal sections. After incubation in 1 % TTC at 37 °C for 30 min, the sections were photographed using a digital camera. White (infarcted) and red (uninfarcted) areas are shown in Fig. 4.

Modified Neurological Severity Scores

Neurological deficits were rated on a scale of 0 to 18 according to the modified neurological severity scores (mNSS) [18]. A higher score represents a more severe infarction. The individual performing the assessment was blinded to the experimental groups of the animals. Scores are expressed as means \pm SE. Two-tailed Student's *t* tests were used for comparisons. Differences were considered significant when $P < 0.05$.

Western Blotting Assay of Apoptosis-Related Factors

The affected side of the cortex was homogenized in PBS or radioimmunoprecipitation assay (RIPA) lysis buffer (Beyotime) at a weight-to-volume ratio of 1:9. The homogenate was centrifuged at 2500 rpm for 10 min at 4 °C, and the protein concentration was assayed using the bicinchoninic acid (BCA) protein assay (Pierce, Rockford, USA). Equal amounts of protein samples were loaded in each lane and electrophoresed in a 15 % separation gel at 120 V (Mini-Protein III Electrophoresis System, Bio-Rad, USA) for 1 h. Proteins from gels were transferred at 200 mA for 80 min onto a nitrocellulose filter membrane. The membranes were incubated overnight at 4 °C with rabbit anti-Bax monoclonal antibody (1:1000 dilution, Abcam, Corp., USA), rabbit anti-Bcl-2 polyclonal antibody (1:1000 dilution, Chemicon International, Inc., USA), rabbit anti-cytochrome c antibody (1:1000 dilution, Cell Signaling Technology, USA), goat polyclonal- β -actin antibody (1:1000 dilution, Santa Cruz, Inc., USA), and then with secondary antibodies diluted at 1:1000 for 1 h at RT. The bands were revealed using enhanced chemiluminescence detection reagents (Pierce). Protein bands were quantified by densitometry (Smartscape, Furi Co., Shanghai, China).

Measurement of Antioxidant Enzyme Activity, Hydrogen Peroxide, and Malondialdehyde Content

The sample proteins were extracted as described above. **The enzyme activity and concentrations of hydrogen peroxide (H_2O_2) and malondialdehyde (MDA) were assessed in the cortex homogenates according to the manufacturer's instructions (BioTNT, Shanghai, China).**

Measurement of Oxidative-Stress-Related Biomarkers

SOD, H_2O_2 , and *T-AOC*

The supernatant was extracted for subsequent testing. All of the operations mentioned above were carried out at 4 °C or on ice. Activity of superoxide dismutase (SOD) was measured at 550 nm and was defined as the rate of inhibition of nitrite reduction by a xanthine–xanthine oxidase system (Sun et al. 1988). To calculate the actual concentration of H_2O_2 , a

standard curve was constructed according to the kit instructions. The total antioxidant capacity (T-AOC) values of the cells were determined using an analysis kit (Beyotime) following the manufacturer's instructions. The final value was quantified by measuring the absorbance at 550 nm, and the relative T-AOC values of the samples were normalized to the protein concentration.

ROS

The fluorescent probe 2',7' dichlorofluorescein diacetate (DCFH-DA) in the Reactive Oxygen Species Assay Kit was used for reactive oxygen species (ROS) detection. DCFH-DA can freely pass through the cell membranes, and then, DCFH is generated through hydrolysis by intracellular esterase. Because DCFH cannot traverse the membrane, the probe can be easily loaded into the cell. Intracellular ROS can oxidize the non-fluorescent DCFH into 2',7' dichlorofluorescein (DCF). DCF fluorescence detection allows for the determination of intracellular ROS levels. Briefly, DCFH-DA was diluted at 1:1000 to a final concentration of 10 mM. Samples were incubated at 37 °C for 20 min and then mixed every 3–5 min so that the probe and the cells were in full contact, followed by washing three times to remove the unbound fraction of DCFH-DA. Fluorescence intensity was determined with a 488-nm excitation wavelength and a 525-nm emission wavelength.

GSH-Px

Tissue extracts were centrifuged at 12,000g for 10 min at 4 °C. Glutathione peroxidase (GSH-Px) activity was measured in the supernatant using a Glutathione Peroxidase Assay Kit (Beyotime, China), which measures the coupled oxidation of nicotinamide adenine dinucleotide phosphate (NADPH) during glutathione reductase (GR) recycling of oxidized glutathione from the GSH-Px-mediated reduction of t-butyl peroxide. In the assay, excess GR, glutathione, and NADPH were added according to the methods recommended by the manufacturer.

Catalase

Catalase (CAT) catalyzes the reduction of H₂O₂ and oxygen to produce water. Residual H₂O₂ can be catalyzed by peroxidase, and the oxidized chromogenic substrate N-(4-antipyrine)-3-chloro-5-sulfonate-p-benzoquinonemonoimine can be generated; the maximum absorption wavelength of this substrate is 520 nm. H₂O₂ standards are used to generate a standard curve, after which the volume of H₂O₂ that has been catalyzed into water and oxygen can be calculated; this process is similar to the detection of H₂O₂ mentioned above. Thus, catalase enzyme activity can be determined. The definition of one unit of catalase enzyme activity is the catalysis of 1 μmol of zymolyte at 25 °C and pH 7.0 in 1 min.

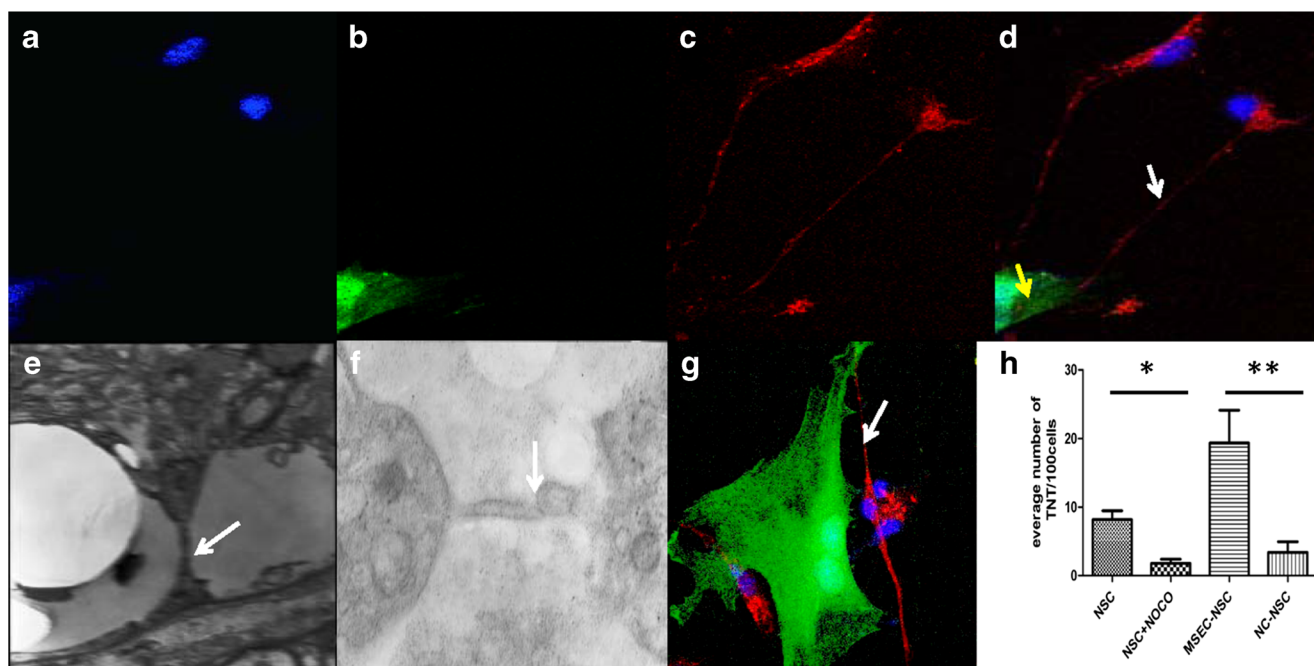


Fig. 1 Cell experiments of TNTs. **a–d, g** Confocal images of TNTs. BMECs or NSCs were labeled with either CFSE (green) or MitoTracker Red (red). MitoTracker Red-labeled cells were co-cultured for 24 h with CFSE-labeled cells. Confocal microscopy revealed mitochondria in the lumens of the TNTs formed between NSCs and BMECs. **e, f** TEM shows a TNT channel (white arrow) connecting NSCs and

BMECs in vitro. **h** The average number of TNT connections in 24 h co-cultures that were untreated or treated with nocodazole or M-sec is shown; $n=6$ per group. *Significant differences between the NSC+PBS and NSC+NOCO groups; **significant differences between the MSEC-NSC and NC-NSC groups

MDA

The Lipid Peroxidation MDA Assay Kit (Beyotime) is based on the chromogenic reaction between MDA and thiosulfate barbituric acid (thiobarbituric acid (TBA)). MDA reacts with TBA at high temperatures in acidic environments to form the MDA-TBA adduct, which has a maximum absorbance at 535 nm. Colorimetry can thus be used for the quantitative detection of MDA in tissue lysates. The weight of the tissue sample accounted for 10 % of the lysis solution. Following a 1600g centrifugation for 10 min, the supernatant was collected for subsequent testing. A 0.1 ml volume of PBS was added to the centrifuge tube to act as blank control, while 0.1 ml aliquots of standards with different concentrations were added to construct the calibration curve. Then, 0.1 ml of each tissue sample was added for measurement, followed by 0.2 ml of the MDA test fluid. After mixing, the samples were boiled in a water bath for 15 min. The water bath was cooled to RT, and the samples were centrifuged at 1000g for 10 min at RT. Aliquots of 200 μ l of the supernatant were added to a 96-well plate followed by measurement of the absorbance at 532 nm with a microplate reader.

Results

TNT Formation Between NSCs and BMECs

Given the recent discovery of TNTs, we investigated whether this type of cell-to-cell communication exists between NSCs and BMECs. TNTs mediate the intercellular transport of mitochondria by generating membrane continuity between cells [19]. We assessed the hypothesis that mitochondria are transported via TNTs. By inhibiting or stimulating the formation of TNTs in cells via the application of specific inhibitors (nocodazole) or activators (M-sec), we expected to observe an altered number of TNTs between cells (Fig. 1h). The average number of TNT connections in 24 h co-cultures that were treated with nocodazole or NC-NSCs was decreased compared with cells without nocodazole pretreatment or cells overexpressing LV-M-sec (1.80 ± 0.58 vs. 8.20 ± 1.28 ; 3.40 ± 1.57 vs. 19.40 ± 4.72 , respectively, $P < 0.05$, Fig. 1h). This result shows that TNTs allow the direct transfer of mitochondria between NSCs and BMECs through cell-to-cell communication (Fig. 1a–g).

In Vivo Effects of Nocodazole and M-sec on MCAO

First, the NSCs and BMECs were close in space (Fig. 2a, b). MitoTracker Red-labeled cells were transplanted via

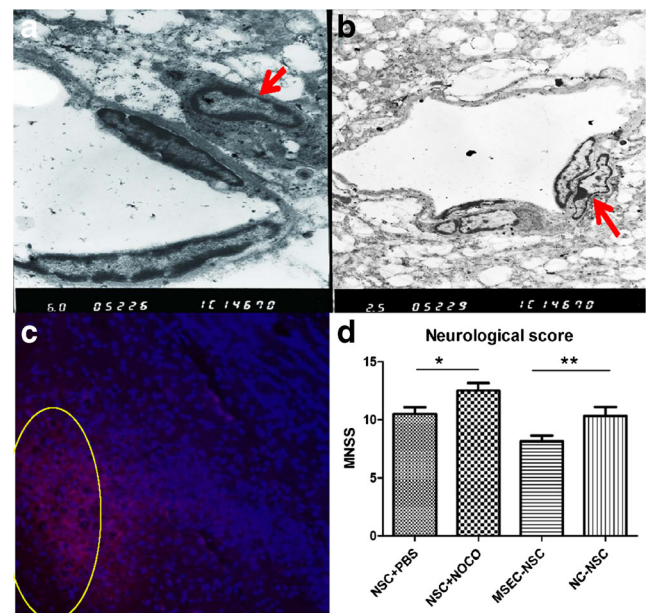


Fig. 2 TEM presentation of TNT and behavioral experiment. **a, b** TEM reveals NSCs (red arrows) and BMECs adjacent to the injury site in vivo. **c** MitoTracker Red-labeled cells were transplanted via intracarotid injection and were noted in the penumbrae of mice subjected to MCAO; nuclear staining is indicated in blue (DAPI). **d** Animals treated with NSC+PBS showed enhanced neurobehavioral function compared with the NSC+NOCO group ($P < 0.05$). MSEC+NSC group animals showed enhanced neurological functional scores at 24 h compared with NC+NSC group animals ($P < 0.05$). *Significant differences between the NSC+PBS and NSC+NOCO groups; **significant differences between the MSEC+NSC and NC+NSC groups

intracarotid injection and observed in the penumbrae of mice subjected to MCAO (Fig. 2c). TNTs are membranous, tubulin-rich structures between cells. Previous studies using MCAO have demonstrated that NSCs improve brain function. The observed effect of NSCs was less pronounced in animals receiving nocodazole-pretreated NSCs and was enhanced in animals receiving NSCs overexpressing LV-M-sec. These indices are illustrated in Figs. 3, 4, and 5.

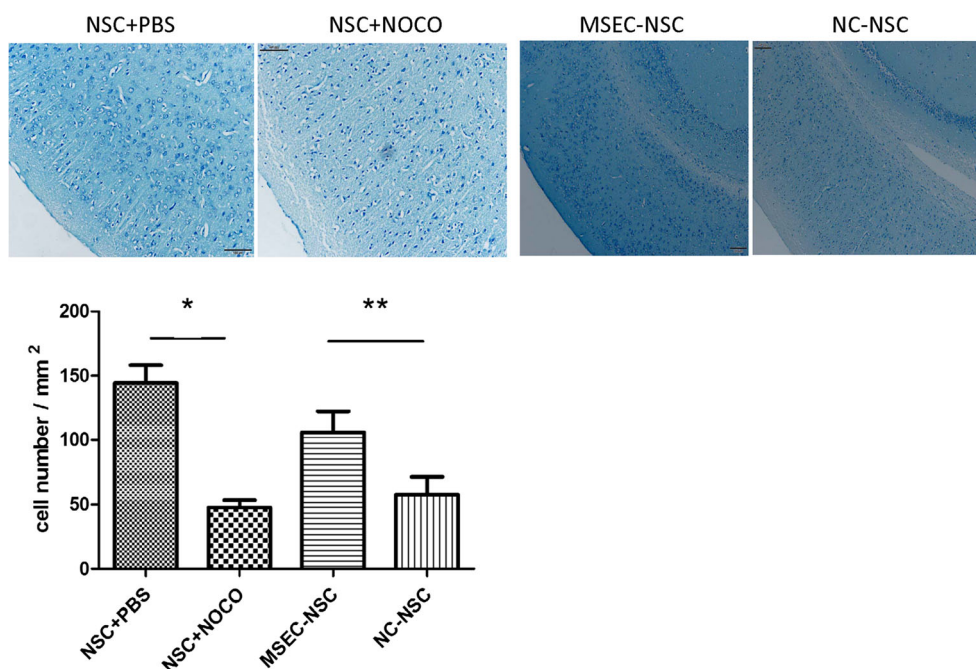
mNSS

Animals treated with NSC+PBS showed enhanced neurobehavioral function compared with the NSC+NOCO group (10.50 ± 0.56 vs. 12.50 ± 0.67 , respectively, $P < 0.05$, Fig. 2d). MSEC+NSC animals exhibited enhanced neurological functional scores at 24 h compared with NC+NSC animals (10.33 ± 0.76 vs. 8.17 ± 0.45 , $i < 0.05$, Fig. 2d).

Nissl Staining

Figure 3 shows representative images of Nissl staining of the cortex at 24 h after MCAO. Larger numbers of intact neurons were noted in the penumbrae of the NSC+PBS

Fig. 3 Nissl staining of the penumbrae. Greater numbers of intact neurons were observed in the NSC+PBS and MSEC-NSC groups. The number of intact neurons per square millimeter in the penumbrae of the NSC+PBS group was increased compared with the NSC+NOCO group ($P<0.01$). The number of intact neurons in the MSEC-NSC group was increased compared with the NC-NSC group ($P<0.05$ for penumbrae); $n=6$ per group. *Significant differences between the NSC+PBS and NSC+NOCO groups; **significant differences between the MSEC-NSC and NC-NSC groups



and MSEC-NSC groups. The number of intact neurons per square millimeter in the penumbrae of the NSC+PBS group was significantly increased compared with the NSC+NOCO group (144.20 ± 14.14 vs. 47.67 ± 5.78 ,

$P<0.01$). The number of intact neurons in the MSEC-NSC group was increased compared with the NC-NSC group (105.80 ± 16.55 vs. 57.67 ± 13.80 , $P<0.05$ for the penumbrae).

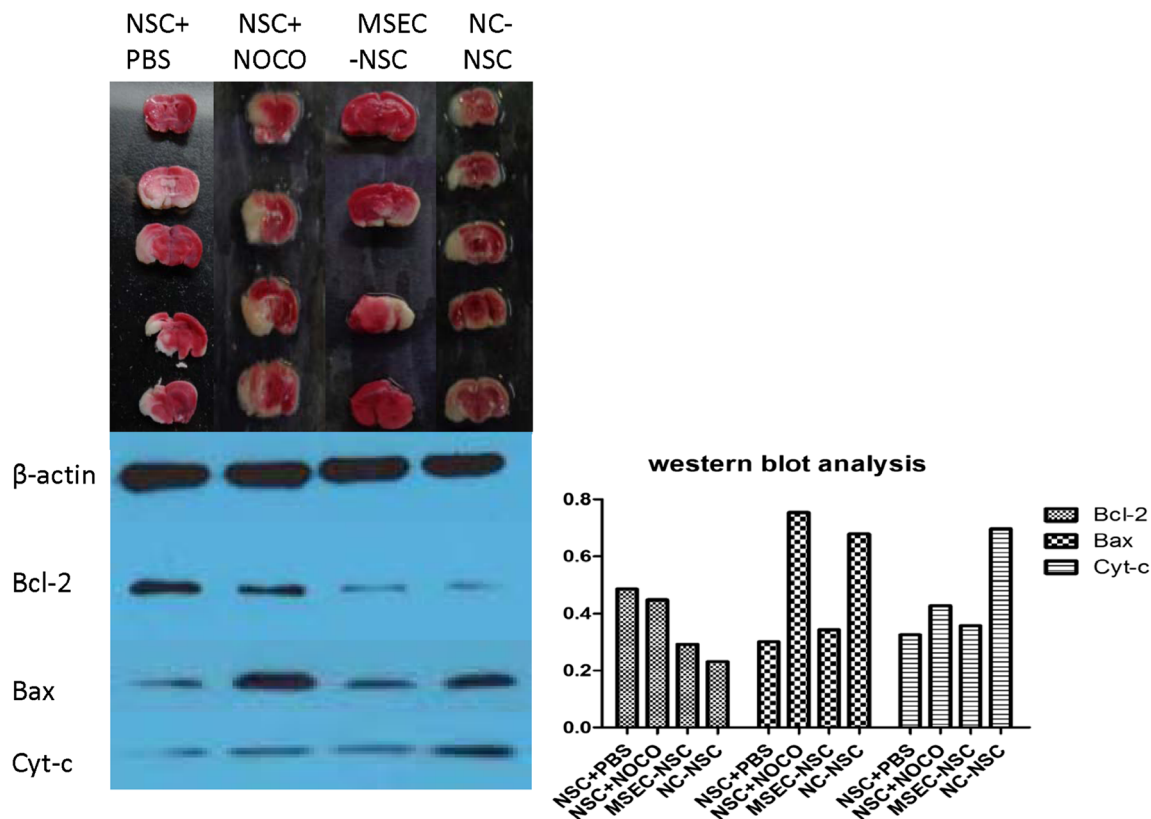


Fig. 4 TTC staining and Western blot analysis of apoptosis-associated factors levels. The NSC+PBS and MSEC-NSC groups showed decreased expression of cytochrome c and Bax in the cortex. Bcl-2 levels were

increased in the NSC+PBS and MSEC-NSC groups compared with their respective control groups. The TTC and Western blot results showed trends of upregulation and downregulation in different groups

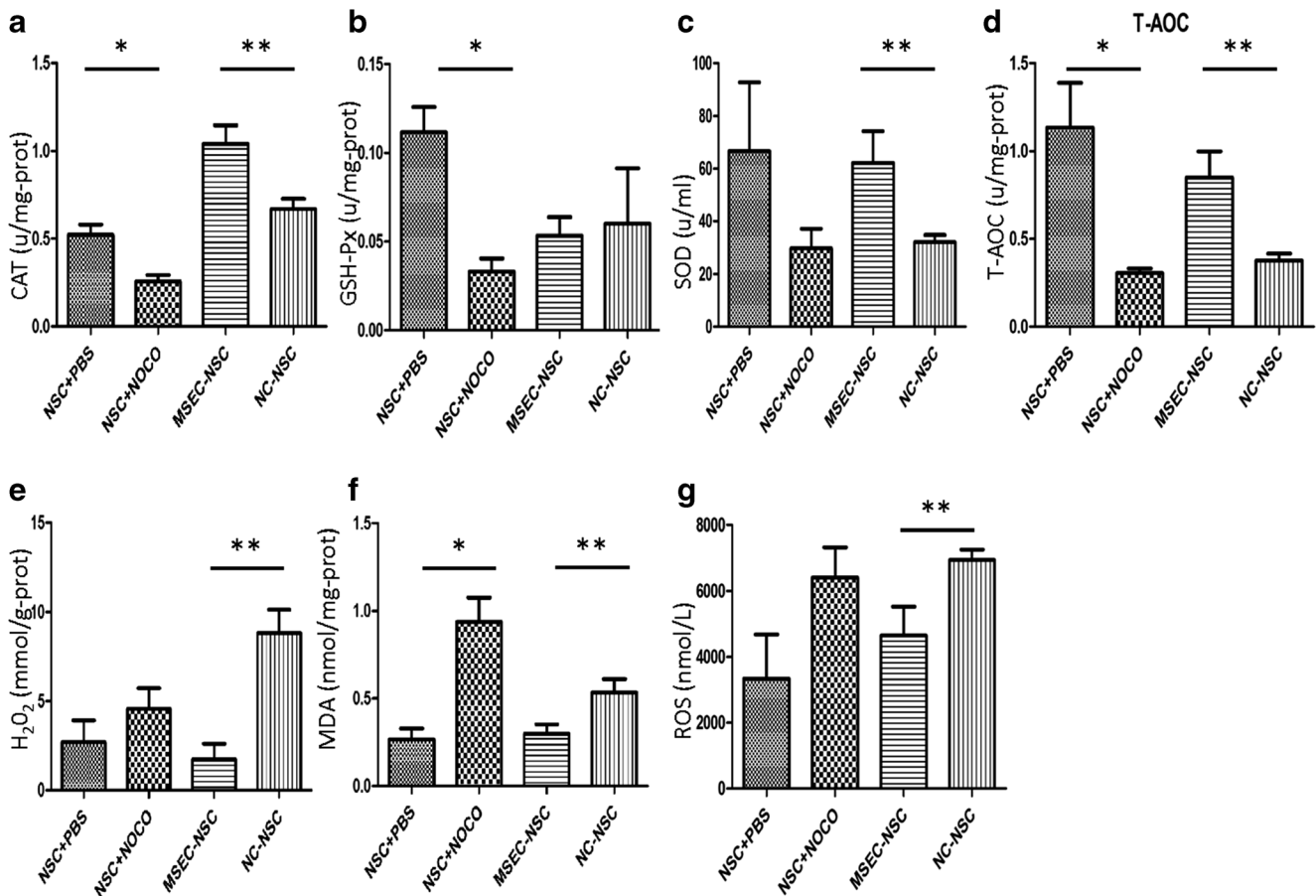


Fig. 5 Activity and content of antioxidant enzymes and ROS. **a** Catalase (CAT). **b** Glutathione peroxidase (GSH-Px). **c** Superoxide dismutase (SOD). **d** Total antioxidant capacity (T-AOC). **e** Hydrogen peroxide (H_2O_2). **f** Malondialdehyde (MDA). **g** Reactive oxygen species (ROS). The CAT, GSH-Px, and T-AOC activity levels in the cortices in the NSC+PBS group compared with the NSC+NOCO group ($*P < 0.05$). The CAT, SOD, and T-AOC activity levels in the MSEC-NSC group compared with

the NC-NSC group ($**P < 0.05$). Regarding peroxidation factors, differences in the H_2O_2 or ROS levels were observed in the cortices of the NSC+PBS and NSC+NOCO groups at 24 h, with the exception of MDA. Compared with the NC-NSC group, the GSH-Px, MDA and ROS activity levels in the MSEC-NSC group ($P < 0.05$); $n = 6$ per group. *Significant differences between the NSC+PBS and NSC+NOCO groups; **significant differences between the MSEC-NSC and NC-NSC groups

Antioxidant Enzyme Activities, Western Blotting, and TTC Staining

The TTC and Western blot results showed trends of upregulation and downregulation in different groups (Fig. 4). At 24 h after ischemia/reperfusion injury, the CAT, GSH-Px, and T-AOC activity levels in the cortices in the NSC+PBS group were increased compared with the NSC+NOCO group (0.52 ± 0.06 vs. 0.26 ± 0.04 ; 0.11 ± 0.01 vs. 0.03 ± 0.01 ; 1.14 ± 0.25 vs. 0.31 ± 0.03 , respectively, $P < 0.05$). No significant difference in SOD activity was observed between these two groups (66.68 ± 25.99 vs. 29.77 ± 7.33 , respectively, $P > 0.05$). The CAT, SOD, and T-AOC activity levels were increased in the MSEC-NSC group compared with the NC-NSC group (1.04 ± 0.11 vs. 0.67 ± 0.06 ; 62.32 ± 11.96 vs. 32.11 ± 2.65 ; 0.85 ± 0.15 vs. 0.38 ± 0.04 , respectively, $P < 0.05$), but the GSH-Px activity was not affected.

Regarding peroxidation factors, no significant differences in H_2O_2 or ROS levels were observed between the cortices of the NSC+PBS group and the NSC+NOCO group at 24 h, but the MDA levels were increased significantly with the addition of nocodazole (0.27 ± 0.06 vs. 0.94 ± 0.14 , respectively, $P < 0.05$). Compared with the NC-NSC group, the H_2O_2 , MDA and ROS levels were significantly decreased in the MSEC-NSC group (1.72 ± 0.89 vs. 8.80 ± 1.33 ; 0.30 ± 0.05 vs. 0.54 ± 0.08 ; $4,650 \pm 879.6$ vs. $6,945 \pm 317.4$, respectively, $P < 0.05$) as detailed in the legend of Fig. 5.

Discussion

NSCs represent a useful tool for research in neural development and function [20] and hold great potential for the treatment of a variety of neurodegenerative and neurotraumatic

diseases. NSCs can self-renew, differentiate into neurons and glial cells, and display a very low risk of malignant transformation [21]. They represent a promising therapy for cerebral ischemia, and our observations suggest that they can abrogate the effects of ROS formation and inhibit apoptosis mediators through TNT formation, augmenting their neuroprotective role. As long membrane tethers between cells, TNTs create supracellular structures that “pull them closer” and “cut-through” them [22], allowing the formation of local networks and favorable microenvironments between groups of cells that enable them to act in a synchronized manner [23]. Thus, complex and specific messages can be transmitted among multiple cells [24], and the strength of the signal suffers relatively little from the distance traveled compared with approaches that involve soluble factors to transmit messages. Because the therapeutic effects of NSCs are likely to depend on paracrine mechanisms mediated by the release of growth factors, anti-apoptotic molecules and anti-inflammatory cytokines to create a favorable environment for the regeneration of neurons, remyelination and improved cerebral flow, narrowing the distance between NSCs facilitates their role in an easier and more effective manner. Transmembrane proteins and membrane-binding proteins, such as N-cadherin and myosin X, are considered necessary in the recognition of, and attachment to, target cells during TNT formation [25].

Mitochondrial exchange between cells via TNTs was demonstrated by electron microscopy together with fluorescence staining in our study, and the present data demonstrate the presence of alpha-synuclein (alpha-syn) within TNTs. As a hypothesis, alpha-syn may enter mitochondria to “pull” them out in an actomyosin-dependent way [26].

The ability of BMECs to induce NSCs to form TNTs implies that this mechanism could be utilized in areas of IS injury. NSCs have long been considered as a potential treatment for IS. We investigated a novel mechanism behind this treatment for subsequent *in vivo* studies.

Direct intralateroventricular injection of cells requires craniotomy via an electrical drill; this technique results in serious traumatic injury. Compared with intralateroventricular and intravenous injections, intracarotid injection exhibits particular advantages and directly contributes to cell-to-cell contact, which induces TNT formation [8], and carries a smaller risk of death in animal models than intralateroventricular injection.

Previous studies indicate that TNTs connecting NSCs are composed of microtubules and F-actin [27], which are important labeling targets in TNT imaging and also play a crucial role in the formation of TNTs. As shown in our experiments, we found that incubation with nocodazole inhibits the polymerization of the microtubule components of TNTs. As expected, the average number of TNT connections decreased dramatically after the NSCs were pretreated (see the [Supplementary figure](#)). Nocodazole is a chemotherapeutic agent, and there is a relationship between vascular injury

and the application of chemotherapeutic agents in humans [28]. The inhibition of TNT formation may serve as a potential exacerbating factor in antitumor drug-induced IS.

M-sec is a central factor in the induction of plasma membrane protrusion during TNT formation. It was first identified as a tumor necrosis factor (TNF) clone from TNF α -stimulated endothelium [29]. Our study showed that TNT formation was enhanced when M-sec expression was upregulated by lentiviral transfection; the ral-exocyst pathway was involved in this process. A more thorough study to elucidate the exact mechanisms might provide further clues and wide-ranging insights into understanding the formation, maintenance and regulation of intercellular transport [30].

In conclusion, our study offers new perspectives on the mechanisms involved in the protective activities of NSCs against IS and supports the interesting possibility that the reparative capacities of NSCs can be enhanced by exogenously manipulating TNT formation. This new principle of intercellular communication is rapidly being explored because it may provide a fast and selective information highway for the coordination of cell migration. Increased understanding of membrane bridges will lead to insights into the basic mechanisms of cellular cross-talk and to the identification of new targets for future, cell-based therapeutic strategies for neuronal diseases.

Acknowledgments This work was supported by the National Natural Science Foundations of China (81230027, 81070959, 81471219), the Outstanding Subject Leaders Project of Shanghai (14XD1403400), Technology Support Project of Shanghai (14140903300), and the Science Committee Animal Project of Shanghai (13140903400).

Conflicts of Interest The authors of this manuscript have no conflicts of interest.

References

1. Ciccone A et al (2013) Endovascular treatment for acute ischemic stroke. *N Engl J Med* 368:904–913. doi:10.1056/NEJMoa1213701
2. Stone LL, Grande A, Low WC (2013) Neural repair and neuroprotection with stem cells in ischemic stroke. *Brain Sci* 3:599–614. doi:10.3390/brainsci3020599
3. Maciaczyk J, Singec I, Maciaczyk D, Klein A, Nikkhah G (2009) Restricted spontaneous *in vitro* differentiation and region-specific migration of long-term expanded fetal human neural precursor cells after transplantation into the adult rat brain. *Stem Cells Dev* 18:1043–1058. doi:10.1089/scd.2008.0346
4. Sakata H et al (2012) Interleukin 6-preconditioned neural stem cells reduce ischaemic injury in stroke mice. *Brain J Neurol* 135:3298–3310. doi:10.1093/brain/awz259
5. Mudo G et al (2009) The FGF-2/FGFRs neurotrophic system promotes neurogenesis in the adult brain. *J Neural Trans* 116:995–1005. doi:10.1007/s00702-009-0207-z
6. Hankey GJ, Eikelboom JW (1999) Homocysteine and vascular disease. *Lancet* 354:407–413. doi:10.1016/s0140-6736(98)11058-9

7. Marzo L, Gousset K, Zurzolo C (2012) Multifaceted roles of tunneling nanotubes in intercellular communication. *Front Physiol* 3:72. doi:10.3389/fphys.2012.00072
8. Rustom A, Saffrich R, Markovic I, Walther P, Gerdes HH (2004) Nanotubular highways for intercellular organelle transport. *Science* 303:1007–1010. doi:10.1126/science.1093133
9. Plotnikov EY et al (2008) Cell-to-cell cross-talk between mesenchymal stem cells and cardiomyocytes in co-culture. *J Cell Mol Med* 12:1622–1631. doi:10.1111/j.1582-4934.2007.00205.x
10. Acquistapace A et al (2011) Human mesenchymal stem cells reprogram adult cardiomyocytes toward a progenitor-like state through partial cell fusion and mitochondria transfer. *Stem Cells* 29:812–824. doi:10.1002/stem.632
11. Bloemendal S, Kuck U (2013) Cell-to-cell communication in plants, animals, and fungi: a comparative review. *Naturwissenschaften* 100:3–19. doi:10.1007/s00114-012-0988-z
12. Koyanagi M, Brandes RP, Haendeler J, Zeiher AM, Dimmeler S (2005) Cell-to-cell connection of endothelial progenitor cells with cardiac myocytes by nanotubes: a novel mechanism for cell fate changes? *Circ Res* 96:1039–1041. doi:10.1161/01.RES.0000168650.23479.0c
13. Figeac F et al (2014) Nanotubular crosstalk with distressed cardiomyocytes stimulates the paracrine repair function of mesenchymal stem cells. *Stem Cells* 32:216–230. doi:10.1002/stem.1560
14. Hase K et al (2009) M-Sec promotes membrane nanotube formation by interacting with Ral and the exocyst complex. *Nat Cell Biol* 11:1427–1432. doi:10.1038/ncb1990
15. Bonner JF, Haas CJ, Fischer I (2013) Preparation of neural stem cells and progenitors: neuronal production and grafting applications. *Method Mol Biol* 1078:65–88. doi:10.1007/978-1-62703-640-5_7
16. Connolly ES Jr, Winfree CJ, Stern DM, Solomon RA, Pinsky DJ (1996) Procedural and strain-related variables significantly affect outcome in a murine model of focal cerebral ischemia. *Neurosurgery* 38:523–531, **discussion 532**
17. Hata R et al (1998) A reproducible model of middle cerebral artery occlusion in mice: hemodynamic, biochemical, and magnetic resonance imaging. *J Cereb Blood Flow Metabol* 18:367–375. doi:10.1097/00004647-199804000-00004
18. Chen CC et al. (2014) A forced running wheel system with a microcontroller that provides high-intensity exercise training in an animal ischemic stroke model. *Braz J Med Biol Res* 47:858–868. doi:10.1590/1414-431X20143754
19. Gurke S, Barroso JF, Gerdes HH (2008) The art of cellular communication: tunneling nanotubes bridge the divide. *Histochem Cell Biol* 129:539–550. doi:10.1007/s00418-008-0412-0
20. Suksuphew S, Noisa P (2015) Neural stem cells could serve as a therapeutic material for age-related neurodegenerative diseases. *World J Stem Cell* 7:502–511. doi:10.4252/wjsc.v7.i2.502
21. Stenudd M, Sabelstrom H, Frisen J (2015) Role of endogenous neural stem cells in spinal cord injury and repair. *JAMA Neurol* 72:235–237. doi:10.1001/jamaneurol.2014.2927
22. Austefjord MW, Gerdes HH, Wang X (2014) Tunneling nanotubes: diversity in morphology and structure. *Commun Integ Biol* 7, e27934. doi:10.4161/cib.27934
23. Minuth WW, Denk L (2015) When morphogenetic proteins encounter special extracellular matrix and cell-cell connections at the interface of the renal stem/progenitor cell niche. *Anatom Cell Biol* 48:1–9. doi:10.5115/acb.2015.48.1.1
24. Abounit S, Zurzolo C (2012) Wiring through tunneling nanotubes—from electrical signals to organelle transfer. *J Cell Sci* 125:1089–1098. doi:10.1242/jcs.083279
25. Lee JY (2014) New and old roles of plasmodesmata in immunity and parallels to tunneling nanotubes. *Plant Sci Int J Exp Plant Biol* 221–222:13–20. doi:10.1016/j.plantsci.2014.01.006
26. Zhang J, Zhang Y (2013) Membrane nanotubes: novel communication between distant cells. *Sci China Life Sci* 56:994–999. doi:10.1007/s11427-013-4548-3
27. Luchetti F et al (2012) Fas signalling promotes intercellular communication in T cells. *PLoS One* 7, e35766. doi:10.1371/journal.pone.0035766
28. Mulrooney DA, Blaes AH, Duprez D (2012) Vascular injury in cancer survivors. *J Cardiovasc Transl Res* 5:287–295. doi:10.1007/s12265-012-9358-7
29. Ohno H, Hase K, Kimura S (2010) M-Sec: emerging secrets of tunneling nanotube formation. *Commun Integ Biol* 3:231–233
30. Gerdes HH, Rustom A, Wang X (2013) Tunneling nanotubes, an emerging intercellular communication route in development. *Mech Dev* 130:381–387. doi:10.1016/j.mod.2012.11.006